Insulin resistance and metabolic hepatocarcinogenesis with parent-of-origin effects in AxB mice

Ian N. Hines,[1] Hadley J. Hartwell,[2,3] Yan Feng,[4] Elizabeth J. Theve,[4] Gregory A. Hall,[4] Sara Hashway,[4] Jessica Connolly,[4] Michelle Fecteau,[4] James G. Fox[4*] and Arlin B. Rogers[2,3*]

[1]Department of Nutrition Sciences, East Carolina University, Greenville, NC; [2]Lineberger Comprehensive Cancer Center, [3]Department of Pathology and Laboratory Medicine, University of North Carolina, Chapel Hill, NC, [4]Division of Comparative Medicine, Massachusetts Institute of Technology, Cambridge, MA. *J.G.F. and A.B.R. share senior authorship.

Text pages: 18

Tables: 3

Figures: 4

Running head: Insulin resistance and HCC in AxB mice

Corresponding author: Arlin B. Rogers, DVM, PhD, Campus Box 7431, University of North Carolina, Chapel Hill, NC 27599-7431; Phone (919) 843-8088, Fax (919) 966-7911, Email abr@med.unc.edu.

Conflicts of interest: None.

Abstract

Insulin resistance is a defining feature of metabolic syndrome and type 2 diabetes but also may occur independently. Nonalcoholic fatty liver disease (NAFLD), the hepatic manifestation of these disorders, increases risk of hepatocellular carcinoma (HCC). However, mechanisms linking hyperinsulinemia to NAFLD and HCC require clarification. Here, we describe a novel mouse model of primary insulin resistance and HCC with strong parent-of-origin effects. Male AB6F1 (A/JCr dam x C57BL/6 sire) but not B6AF1 (B6 dam x A/J sire) mice developed spontaneous insulin resistance, NAFLD and HCC without obesity or diabetes. A survey of mitochondrial, imprinted, and sex-linked traits revealed modest associations with X-linked genes. However, a diet-induced obesity study including B6.A chromosome substitution-strain (consomic) mice showed no segregation by sex chromosome. Thus, parent-of-origin effects were specified within the somatic genome. Next, we interrogated mechanisms of insulin-associated hepatocarcinogenesis. Steatotic hepatocytes exhibited adipogenic transition characterized by vacuolar metaplasia and upregulatation of vimentin, adipsin, fatty acid translocase (CD36), perosixome proliferator-activated receptor-γ, and related genes. This profile was largely recapitulated in insulin-supplemented primary mouse hepatocyte cultures. Importantly, pyruvate kinase M2, a fetal anabolic enzyme implicated in the Warburg Effect, was activated by insulin in vivo and in vitro. In summary, our study reveals parent-of-origin effects in heritable insulin resistance, and implicates adipogenic transition with acquired anabolic metabolism in the progression from NAFLD to HCC.

Introduction

Metabolic diseases such as obesity, insulin resistance, metabolic syndrome and type 2 diabetes (T2D) are reaching epidemic proportions.[1] Serious co-morbidities are associated with these conditions including hypertension, cardiovascular disease and increased risk for several types of cancer.[2, 3] Nonalcoholic fatty liver disease (NAFLD), the hepatic manifestation of this group of disorders, increases the risk of hepatocellular carcinoma (HCC).[4] HCC is the 3rd leading cause of cancer deaths worldwide, and the fastest rising cancer in the United States.[5] In a recent prospective study of asymptomatic U.S. middle-aged adults, the prevalence of NAFLD by ultrasound and/or biopsy was found to be 46%.[6] Nonalcoholic steatohepatitis (NASH), the more serious NAFLD subcategory defined by hepatic steatosis, inflammation and ballooning degeneration, afflicts 12% of middle-aged Americans.[6] As a result, NAFLD/NASH may one day surpass hepatitis C virus infection as the leading cause of HCC in this country.

Genetic predisposition contributes to HCC risk on a metabolic background, but molecular markers of preneoplastic progression and hepatocellular transformation remain elusive. Moreover, due to extensive overlap in clinical presentation, it is difficult to ascribe hepatic consequences such as NAFLD and HCC to specific metabolic triggers. Existing animal models of metabolic hepatopathy are ill-equipped to address these questions because most exhibit obesity, insulin resistance and/or T2D as part of a disease continuum. New models are needed to dissect the roles of individual metabolic parameters in the pathogenesis of hepatic steatosis and carcinogenesis. Here, we report a novel mouse model of primary insulin resistance and NAFLD leading to HCC in the absence of obesity or T2D. Intriguingly, the model exhibits strong parent-of-origin effects encoded predominantly within the somatic genome, suggesting involvement of

3

imprinted genetic elements that may serve as useful biomarkers and/or interventional targets. We used this model to probe mechanisms of hyperinsulinemic NAFLD and HCC, and documented adipogenic transition of hepatocytes with reactivation of the anabolic enzyme pyruvate kinase M2, a fetal proto-oncogene associated with the Warburg Effect.[7] Taken together, our results suggest that epistatic interactions between parent-specific loci play an important role in regulating insulin sensitivity, and that hepatocellular adipogenic transition with acquired anabolic metabolism represents a potential mechanistic link between NAFLD and HCC.

Materials and Methods

Animals and Study Design

A/JCr mice (A/J) were purchased from the National Cancer Institute (Frederick, MD). C57BL/6J (B6) and B6.A chromosome substitution-strain (CSS; consomic) mice were obtained from the Jackson Laboratory (Bar Harbor, ME). Experiments were performed in facilities accredited by the Association for Assessment and Accreditation of Laboratory Animal Care. Mice were maintained in static microisolator cages under specific pathogen-free conditions for 11 murine viruses, *Helicobacter* spp., *Salmonella* spp., *Citrobacter rodentium*, ectoparasites and endoparasites. *Helicobacter*-free status was confirmed by DNA PCR on pooled cage feces.[8] In the first experiment, A/J and B6 mice were intercrossed and parent-of-origin records maintained to identify offspring as AB6F1 or B6AF1. All F1 offspring (n=59) were fed the same rodent chow diet (Prolab RMH 3000; Scott's Distributing, Hudson, NH) and collected at 3, 9 or 15 months of age. In a follow-up diet-induced obesity (DIO) study, A/J, C57BL/6J-Chr X$^{A/J}$/NaJ

(B6.AX), C57BL/6J-Chr $Y^{A/J}$/NaJ (B6.AY), AB6F1 and B6AF1 mice were raised under standard conditions until 6 weeks of age and then randomly assigned into low-fat (LF) or high-fat (HF) diet groups (minimum 8 animals per sex per group, n=207). The LF diet contained 10 kcal%fat and the HF diet 60 kcal%fat (catalog numbers D12450B and D12492; Research Diets, New Brunswick, NJ). Mice were maintained on the LF or HF diet for 12 weeks. Mice in both studies were euthanatized via CO_2 inhalation according to recommendations of the AVMA Panel on Euthanasia. Protocols were compliant with the *U.S. Public Health Service Policy on Humane Care and Use of Laboratory Animals*, and approved by the Massachusetts Institute of Technology Committee on Animal Care and University of North Carolina Institutional Animal Care and Use Committee. Body weight was recorded and blood collected via cardiac puncture immediately following euthanasia. Full necropsies were performed and blood and tissues collected per our published protocol.[9]

Blood and tissue analyses

Blood glucose concentrations were obtained using the One Touch Basic glucometer (LifeScan, Milpitas, CA). Cholesterol was measured with the Accutrend GC (Roche Diagnostics, Branchburg, NJ). Serum insulin was determined with the Lincoplex rat/mouse insulin ELISA kit (Millipore, Billerica, MA). The homeostatic model of assessment for insulin resistance (HOMA-IR) was calculated as described.[10] Parametric laboratory data between all groups were compared by one-way analysis of variance (ANOVA) with Tukey post-test, and between pairs by Student t-test using Prism software (GraphPad, San Diego, CA). *P*-values < 0.05 were considered significant. Hematoxylin and eosin-stained slides of liver were graded by a board-certified

veterinary pathologist (A.B.R.) blinded to sample identity for hepatic steatosis based on semi-quantitative percentage of centrilobular and midzonal hepatocytes containing lipid vacuoles: (0) < 5% of hepatocytes, (1) 5-25%, (2) 25-50%, (3) 50-75%, (4) >75%. Macrovesicular and microvesicular steatosis were scored separately according to published morphologic criteria. The combined scores were added to generate a fatty liver index. Inflammation and dysplasia/neoplasia also were scored according to our published criteria.[9] Nonparametric histopathology scores were compared between all groups by Kruskal-Wallis ANOVA with Dunn's post-test, and between pairs by Mann Whitney-U. Frozen liver sections in O.C.T. medium were cryosectioned and stained with oil red O for lipids. Immunohistochemistry for PKM2 (antibody #3198, Cell Signaling Technology, Beverly, MA) was performed on a Bond-III immunostainer (Leica, Bannockburn, IL) following techniques we have published.[11]

Gene expression analysis

mRNA was isolated from liver and assessed for quality as we have previously described.[12] Tissues from two 9-month-old male AB6F1 and B6AF1 mice were analyzed using the Mouse Genome 430A 2.0 Array (Affymetrix, Santa Clara, CA). Data were imported into Partek Genomics Suite (Partek, St. Louis, MO) using Robust Multichip Average, and normalized by response variable. Data were filtered by presence/absence call and P-value (<0.05). Signal fold-changes ≥1.5 were considered significant. The complete data set was deposited in the NIH Gene Expression Omnibus, #GSE26225. Results for selected genes were validated and extended across all groups by SYBR green quantitative RT-PCR (qRT-PCR) as described previously.[13] Primers were designed using MacVector 11 software (Cary, NC). Unique primer sequences are

presented in Table 1; all others as described by Amador-Noguez et al.[14]

Primary hepatocyte isolation and culture

Primary mouse hepatocytes were derived from collagenase-digested 8-week-old male B6 mouse livers, and isolated and cultured following protocols described elsewhere with minor modification.[15] Briefly, murine livers were sequentially perfused *in situ* with 25 mL calcium-free EGTA-containing buffer followed by 50 mL buffered saline containing 0.3 mg/mL Type IV collagenase (Roche Diagnostics Corp, Indianapolis, IN) at 37° C. Following perfusion, collagenase-treated livers were dissociated by mincing with scissors followed by passage through a 100 μm-pore nylon mesh. Hepatocytes were purified via repeated (3X) low-speed (50 x g) centrifugation. Cell purity was assessed by light microscopy and by fluorescence-assisted cell sorting. For the latter, 1×10^5 cells were labeled with anti-CD45/leukocyte-common antigen or anti-Fas (CD95) antibodies (or appropriate conjugated isotype control antibodies, all from eBioscience, San Diego, CA) for 30 minutes at room temperature followed by evaluation on an Accuri C6 Flow Cytometer (Ann Arbor, MI). Purified hepatocytes were grown on collagen I-coated matrices (BD Biocoat, BD Biosciences, Franklin Lakes, NJ) in Dulbecco's modified Eagle medium with 10% fetal bovine serum, penicillin/streptomycin, and 2 mM L-glutamine. Subsets of cells were supplemented with insulin (5 mg/L), transferrin and selenium (ITS) ± dexamethasone (10 mM; both Sigma, St. Louis, MO). After 1 or 4 days, cells were harvested and RNA isolated followed by qRT-PCR as described above. Cell viability was determined using a 3-(4,5-dimethylthiazol-2-yl)-2,5-diphenyltetrazolium bromide (MTT) kit according to the manufacturer's instructions (Molecular Probes, Eugene, OR). For assessment of hepatocyte

morphology, cell suspensions were dropped onto silanized glass slides, fixed in chilled acetone

for 10 min, and stained with Diff-Quik (Fisher Scientific, Pittsburgh, PA).

Results

Insulin resistance without obesity or T2D in AB6F1 male mice

We characterized the phenotype of AxB F1 mice fed a standard rodent chow diet for 3, 9 or 15

months. First, body and liver weights were determined. AB6F1 male mice weighed 15-23%

more than age-matched B6AF1 controls when compared across time points (Fig. 1). Whereas

this difference was statistically significant, AB6F1 mice were not obese and could not be

visually distinguished from BA6F1 males. Female AB6F1 mice also weighed slightly more than

B6AF1 females, but the difference was statistically insignificant (not shown). AxB F1 mice of

both sexes weighed more than published mean body weights for either parental inbred strain

(Mouse Phenome Database, Jackson Laboratory). Thus, hybrid mice were larger than parental

strains, but morbid obesity was not a component of the F1 phenotype. At necropsy, it was noted

that the livers of many males were enlarged and pale. Absolute liver weight and liver:body

weight ratios were found to be greater in AB6F1 than B6AF1 male mice at 9 and 15 months

(Fig. 1). Male AB6F1 had significantly increased serum insulin levels relative to B6AF1 males at

all time points. Nevertheless, despite increased serum insulin levels in AB6F1 males there were

no significant differences in mean blood glucose between any groups regardless of sex or time

point (not shown). Moreover, no animals developed polyuria, polydipsia, hyperphagia and/or

body wasting characteristic of diabetes.[16] Thus, in spite of high circulating insulin levels, AB6F1

mice did not exhibit obesity or T2D. These results demonstrate that AB6F1 but not B6AF1 male mice develop spontaneous hyperinsulinemia on a standard chow diet, and that this insulin resistance is not associated with morbid obesity, metabolic syndrome or T2D.

Hyperinsulinemic NAFLD and HCC in AB6F1 males

Blinded histopathologic assessment of livers from AxB F1 mice revealed mild-to-moderate hepatic steatosis in a subset of animals by 3 months of age, marked steatosis by 9 months, and severe steatosis with dysplasia and/or HCC by 15 months. When the results were decoded, it was confirmed that the most significant lesions arose in hyperinsulinemic AB6F1 males (Fig. 2A). B6AF1 males showed no or minimal liver lesions at 3 and 9 months of age. However, 50% of BA6F1 males did exhibit mild-to-moderate steatosis at 15 months. In AB6F1 males, histologic changes characteristic of insulin resistance were identified in tissues besides the liver as well. These included WAT degeneration with $F4/80^+$ pericellular macrophages forming crown-like rosettes, thoracic BAT metaplasia to a WAT phenotype, focal skeletal muscle degeneration with fatty replacement, and pancreatic islet hyperplasia with occasional megaislets (Fig. 2B). Within the liver, preneoplastic and neoplastic lesions including foci of cellular alteration, dysplastic nodules and HCC were limited to AB6F1 males (30% incidence versus 0% in BA6F1; Fig. 2C). This is significant because spontaneous HCC is very rare in wild-type (WT) A/J and B6 strains within the typical 24-month lifespan (Mouse Phenome Database). Because high insulin levels also have been associated with tumors of the pancreas and lower bowel,[17, 18] we examined those organs grossly and histologically but found no neoplastic or preneoplastic lesions (not shown). Histopathology of female mouse tissues including liver was unremarkable. These findings are

consistent with the male-predominance of metabolic and neoplastic liver disease documented in humans and other rodent models.[6, 19] Viewed together these results demonstrate that hyperinsulinemia, in the absence of morbid obesity, metabolic syndrome or T2D, is sufficient to induce HCC in mice.

NAFLD-associated cytokine induction, acute-phase responses and hepatic feminization

To determine the global impact of hepatic steatosis on gene expression, we performed microarray analysis of liver samples from 9-month-old male AB6F1 and B6AF1 mice. Hierarchal clustering analysis using Partek Genomics Suite demonstrated clear segregation of the two genotypes (Fig. 2D). Four interrelated pathophysiologic processes were evident in the steatotic male AB6F1 liver: inflammation, acute-phase responses (APR), transcriptional feminization, and metabolic derangement. Numerous proinflammatory genes were upregulated including Stat1, IFN-γ-induced GTPases and interferon-activated/regulatory factors, histocompatibility 2 class II antigens, and others (top 10 altered genes Table 2; complete data set available Gene Expression Omnibus #GSE26225). APR induction was confirmed by the upregulation of canonical acute-phase murine genes including lipocalin 2, serum amyloid A1 and A2, orosomucoid, and metallothioneins 1 and 2.[12] Of note, all of these transcriptional changes occurred in the absence of histologic hepatitis, demonstrating that NAFLD produces a morphologically covert pro-inflammatory microenvironment. Nonspecific injury of the male mouse liver frequently leads to loss of gender-specific gene expression characterized by transcriptional feminization.[13] Accordingly, we found a significant bias for sex-dependent gene alterations in the feminine direction in AB6F1 males with NAFLD. Feminine genes up-regulated

in the steatotic male liver included sulfotransferase 2a2 and Sult3a1, cytochrome P450 2b13 (Cyp2b13), lymphocyte antigen 6 complex locus D, ATP-binding cassette D2, fatty acid-binding protein 5 (epidermal), and acyl-CoA thioesterase 3. Simultaneously, masculine genes were downregulated in the male AB6F1 liver including solute carrier organic anion transporter 1a1, hydroxysteroid dehydrogenase 3β-V, elongation of very long chain fatty acids-like 3, elastase-1 (pancreatic), and Cyp7b1. Whereas many of the metabolic gene alterations in AB6F1 male mice were attributable to hepatic feminization, gender-neutral genes associated with metabolic function also were dysregulated including potassium channel T2, complement factor D (adipsin), sulfotransferase 5A1, and insulin-like growth factor binding protein 2. Taken together, these data demonstrate that insulin resistance and NAFLD are sufficient to invoke robust hepatic transcriptional alterations related to inflammation, metabolism and sex-dependent liver function.

Parent-of-origin effects not linked to known maternal/paternal genes

There are three known sources of parent-specific gene expression: mitochondrial DNA, imprinted loci, and sex-linked genes.[20] Genes transcribed from mitochondrial DNA are maternal in origin, imprinted genes are transcribed from a single parental allele, and sex chromosomes are inherited in parent-specific fashion in males. Because of the strong parent-of-origin effects in AxB F1 mice, we interrogated by qRT-PCR genes meeting any of those criteria and shown to be differentially expressed by microarray. Additionally, we analyzed known parent-specific genes canonically associated with metabolism. Altogether, we assessed 4 mitochondrial DNA transcripts, 8 imprinted alleles, and 29 sex-linked genes in all male mice (Table 1). No imprinted or mitochondrially-encoded gene exhibited differential expression between AB6F1 and B6AF1

mice (data not shown). In contrast, four X-linked genes showed a positive correlation with NAFLD at one or more time points. Of these, three were upregulated at 9 and 15 months only (Frmpd3, Slc25a5, Tmsb4x), suggesting an associative rather than causative relationship. The only X-linked gene upregulated at all time points in AB6F1 males was thyroxine-binding globulin (TBG; *Serpina7*). Interestingly, this gene also was increased in B6AF1 males with steatosis at 15 months. However, in all affected animals TBG upregulation was modest (~2-fold) and showed no linear correlation with NAFLD severity (data not shown). Further work will be required to determine whether TBG contributes to the pathogenesis of insulin resistance and NAFLD or is merely a bystander. Viewed as a whole, our PCR survey failed to identify a robust candidate among known uniparentally expressed genes to account for the dramatic parent-specific metabolic phenotype in AxB F1 males, suggesting that the disease is polyfactorial and may involve epigenetic mechanisms.

Gender- and strain-specific responses to high-fat diet in CSS and F1 mice

Because we found some associations between X-linked genes and the AB6F1 metabolic phenotype, we performed a follow-up DIO study using sex chromosome-substitution strain B6.A mice. These animals were on a B6 background except for an A/J-derived sex chromosome.[21] Also included were AxB F1 mice along with a WT A/J control group. An additional control group of WT B6 mice had to be excluded due to poor breeding kinetics resulting in insufficient numbers. In agreement with the first study showing increased BW in AxB F1 mice relative to the parent strains, B6AF1 and AB6F1 mice on the LF diet weighed significantly more than sex-matched A/J and CSS strains (Table 3). All mice on the HF diet weighed significantly more than

sex- and strain-matched animals on the LF diet. However, as a percentage of baseline body mass, CSS mice on the HF diet gained more weight than A/J and F1 mice. This was especially true of B6.AX males, which weighed less than all other male groups on the LF diet, but the same as all but the A/J males on the HF diet. In A/J and CSS mice, serum insulin levels rose in relative proportion to body mass on the HF diet. In stark contrast, insulin levels were significantly lower in B6AF1 and significantly higher in AB6F1 males compared with CSS mice despite nearly identical body weights (Fig. 3). A similar dichotomy between serum insulin and body mass was observed in female F1 mice on the HF diet. Thus, insulin resistance in F1 mice was regulated by distinct mechanisms from those governing diet-induced weight gain. Female CSS and AxB F1 but not A/J mice on the HF diet exhibited mild-to-moderate macrovesicular steatosis that did not vary by strain (data not shown). Male A/J mice on the HF diet developed moderate patchy macrovesicular steatosis, whereas CSS and F1 males developed severe diffuse mixed hepatic steatosis (mean fatty liver index = 5/8; not shown). The proportion of microvesicular-to-macrovesicular steatosis varied within but not between groups. Viewed as a whole, these results demonstrated that weight gain and hepatic steatosis increased in tandem in response to the HF diet, whereas insulin resistance was distinctly regulated in F1 male and female mice. Indeed, B6AF1 were protected from DIO-associated insulin resistance compared with CSS mice, whereas AB6F1 displayed exaggerated hyperinsulinemia in response to caloric overload. This suggests synergy in epistatic interactions between parent-specific alleles in hybrid mice resulting in a marked shift in insulin sensitivity in a positive or negative direction. Taken together, these results show that insulin resistance is not directly correlated with increased body mass, and that additional genetic factors determine the metabolic consequences of diet-induced obesity.

Insulin resistance invoked adipogenic transition of hepatocytes and reactivated PKM2

Because of the remarkable histologic similarity between steatotic hepatocytes and adipocytes (Fig. 2E), we wondered whether fatty liver was associated with molecular changes characteristic of adipogenic transition.[22] By microarray and qRT-PCR, we found numerous examples of adipocyte-associated genes that were upregulated in the livers of 9-month-old AB6F1 mice with NAFLD compared with B6AF1 controls. As mesenchymal cells, adipocytes express a number of canonical genes not typically expressed in hepatocytes and other epithelial tissues. Mesenchymal cell markers that were increased in the livers of mice with NAFLD included vimentin, platelet-derived growth factor-β, and collagen 3α-1 (Fig. 4A and Supplemental Data). Additionally, there was upregulation of more specific adipocyte-associated genes including complement factor D (adipsin), fatty acid translocase (CD36), fatty acid binding protein-4 (adipocyte), and peroxisome proliferator-activated receptor-γ (PPARγ). Of singular importance, the fetal isoform of pyruvate kinase, Pkm2 was upregulated nearly 2-fold in 9-month-old mice with NAFLD. Functional protein expression was confirmed by IHC, where cytoplasmic and nuclear PKM2 localization was visualized in neoplasms from AB6F1 mice, but not in normal B6AF1 liver (Fig. 2A). These results confirm that chronic hyperinsulinemia invokes adipogenic transition of hepatocytes and invokes metabolic pathways in improper context that may contribute to cellular transformation.

Insulin-dependent adipogenic transition and PKM2 activation in cultured hepatocytes

To validate our in vivo findings and confirm that transcriptional alterations reflected changes in parenchymal and not accessory liver cells, we harvested, purified and cultured primary mouse

hepatocytes. To insure purity, we performed FACS analysis which confirmed <2%

contamination by white blood cells (Fig. 4A). Approximately 25% of the purified hepatocytes

were positively labeled with an anti-CD95/Fas antibody, in keeping with the known low level of

Fas surface expression in healthy mouse liver.[23] To insure that our cultured cell population was

primarily hepatocytes, we performed qRT-PCR for albumin and Apoa1 on freshly purified cells

and found gene expression levels similar to those from intact mouse liver RNA (not shown).

Primary hepatocytes grown in the presence of insulin exhibited greater viability after 4 days than

did those grown without insulin supplementation (Fig. 4B). Under all growth conditions, primary

hepatocytes organized into crude canalicular structures; however, insulin-supplemented cells

exhibited clear cytoplasmic lipid-storage vacuoles that were not evident in cells grown in the

presence of dexamethasone alone (Fig. 4B). Insulin supplementation to primary hepatocytes

resulted in upregulation of many of the same adipocyte-associated genes we documented in

AB6F1 mice with NAFLD, including but not limited to vimentin, collagen 3α-1, fatty acid

translocase (CD36) and Pkm2 (Fig. 4C). Taken together, these results confirm that

supraphysiologic levels of insulin promote hepatocyte survival and invoke activation of

adipocyte-associated metabolic pathways that may contribute to cellular transformation.

Discussion

Beneath the current wave of obesity and T2D lurks a larger swell of subclinical metabolic

disease. In some settings, up to 75% of individuals with NAFLD are nonobese.[24] Most diagnoses

of NAFLD in the United States are made in patients without previously identified risk factors.

Indeed, in a recent study, nearly half of clinically healthy middle-aged adults in the U.S.

15

exhibited NAFLD by ultrasound and/or biopsy.[6] The potential impact of covert insulin resistance and NAFLD on a national scale is unknown. However, it is noteworthy that HCC continues to rise in the United States despite flat or declining levels of viral hepatitis and alcoholism. Indeed, NAFLD/NASH may one day surpass HCV infection as the leading cause of liver cancer in the United States.[5]

Because of the complex interactions between metabolic disease and HCC, animal models are needed to characterize the molecular events leading from steatosis to cancer. We observed that male F1 offspring of A/J and B6 mice developed spontaneous insulin resistance, NAFLD and HCC without obesity or T2D. Intriguingly, the model exhibited strong parent-of-origin effects. AB6F1 but not B6AF1 mice developed early onset insulin resistance and NAFLD that progressed to HCC in many by 15 months of age. Despite this parent-of-origin-specific inheritance, we found no strong associations with known uniparentally expressed mitochondrial or imprinted genes, although modest associations with some X-linked genes were suggested. However, a follow-up DIO study involving X and Y CSS mice confirmed no significant phenotypic segregation by sex chromosome, although B6.AX mice did exhibit a leaner metabolic profile than B6.AY mice on the LF diet. We concluded that the strong parent-of-origin effects in AxB F1 mice were specified within the somatic genome. Importantly, the DIO experiment also revealed that obesity and insulin resistance were regulated by distinct genetic mechanisms in hybrid animals.

Diabetes is associated with increased risk of HCC in humans.[25] In diabetic patients, treatment with sulphonylurea or exogenous insulin increases HCC risk and worsens tumor response to

radioablation, whereas HCC patients taking the insulin-sensitizing drug metformin have more favorable outcomes.[26-28] This suggests a direct role for insulin in liver tumor promotion. Because insulin resistance in the absence of obesity or diabetes was sufficient to promote HCC in AB6F1 mice, we investigated potential mechanisms of metabolic hepatocarcinogenesis. In mice with hyperinsulinemic NAFLD, hepatocytes underwent partial adipogenic transition characterized morphologically by vacuolar metaplasia resembling WAT or BAT. At the molecular level, canonical adipocyte genes were activated in steatotic hepatocytes including vimentin, adipsin, fatty acid translocase (CD36), fatty acid-binding protein 4 (adipocyte), stearoyl-coA desaturase 2, and PPAR-γ. This transcriptional profile was largely recapitulated in insulin-supplemented, but not deprived, primary mouse hepatocytes in vitro. Supraphysiologic insulin exposure also promoted hepatocyte survival in culture. Of special significance discussed below, we found that excess insulin reactivated the fetal isoform of pyruvate kinase (PKM2) in hepatocytes both in vitro and in vivo.

Complex metabolic traits are regulated polygenetically.[29] Thus, our inability to pinpoint a single gene that accounted for the parent-specific metabolic phenotype in AxB F1 mice was not surprising. Because neither parental inbred strain develops equivalent disease, polygenetic crosstalk rather than a single gene polymorphism best explains the positive and negative heterosis observed in B6AF1 and AB6F1 males, respectively.[30] Whereas our genomic survey of F1 mice did reveal a modest association between NAFLD and X-linked thyroxine-binding globulin, the follow-up DIO study with CSS mice did not validate phenotypic segregation by sex chromosome. In the original description of B6.A CSS mice, it was noted that 17 of the 23 CSS lines exhibited an intermediate obesity phenotype between parental inbred strains.[21] Thus,

metabolism is governed by multiple genes on an array of different chromosomes. Recent work

has revealed important obesity-related quantitative trait loci on chromosomes 6 and 17.[31, 32]

Others are likely to follow. Combining our results with those from other laboratories, it seems

clear that polygenic epistatic interactions including those inherited in a parent-specific fashion

coordinately regulate insulin sensitivity. These findings take on direct translational significance

in light of a recent study from Iceland showing that parent-specific somatic polymorphisms

strongly influence T2D risk in humans.[33]

In addition to its value as a genetic tool, the AxB mouse model has utility for addressing

molecular mechanisms of hepatocarcinogenesis in the context of primary insulin resistance. For

example, we observed that vacuolated hepatocytes in mice with hyperinsulinemic NAFLD not

only took on a morphologic appearance of WAT or BAT, but also expressed many genes

classically associated with adipose tissue. These included but were not limited to adipsin, fatty

acid translocase, fatty acid binding-protein 4, vimentin and PPARγ. The important role of insulin

in adipogenic transition was confirmed by our *in vitro* experiments that recapitulated the

emergence of lipid vacuoles along with up-regulation of adipogenic genes in primary mouse

hepatocytes. Moreover, we confirmed that insulin extends hepatocyte survival and inhibits

apoptosis. This may have *in vivo* significance, as liver cells undergoing severe oxidative stress in

a pro-inflammatory microenvironment would be prevented from entering apoptosis in the

context of hypersinulinemia, as shown experimentally in skeletal muscle.[34]

A singularly important potential link between hyperinsulinemia, adipogenic transition and HCC

revealed by this study was pyruvate kinase M2. Pyruvate kinases are critical enzymes in

glycolytic oxidative phosphorylation. There are four pyruvate kinase isoforms: L, R, M1 and M2.[35] The adult liver is characterized by expression of the L-type isoform.[36] In contrast, M2 is expressed predominantly during embryogenesis in the fetal liver and other rapidly dividing tissues.[37] In contrast to the adult isoforms, PKM2 diverts glucose metabolism to an alternate pathway that generates short carbon chains for molecular building blocks needed by rapidly dividing cells.[38] Aberrant expression of PKM2 is a common feature of cancers that rely on aerobic gycolysis with lactate generation (Warburg Effect) to support rapid proliferation. Intriguingly, PKM2 is activated normally in an insulin-dependent fashion during the programmed differentiation of NIH 3T3 cells from preadipocytes to adipocytes.[39] It is possible that insulin invokes adipogenic transition and Pkm2 expression in hepatocytes through similar mechanisms. Of note, the only two adult mammalian tissues that ordinarily express PKM2 are skeletal muscle and adipose tissue, both of which are replicatively senescent.[40, 41] In contrast, hepatocytes enter cell division with little prompting. It is tempting to speculate that insulin-directed PKM2 reactivation in replication-competent cells such as hepatocytes represents a significant proto-oncogenic event. If so, PKM2 inhibitors currently under development for the treatment of established cancer also may have utility for the prevention of HCC in patients with insulin resistance and NAFLD.[42] Further study will be required to test this hypothesis.

In summary, we have introduced a novel mouse model of primary insulin resistance, NAFLD and HCC with strong parent-of-origin effects. AB6F1 but not B6AF1 male mice develop spontaneous insulin resistance that leads to severe NAFLD by 9 months and HCC by 15 months. Parent-specific inheritance in this model is polygenetic and encoded within the somatic genome. We have shown that insulin resistance is regulated independently of diet-induced weight gain in

AxB F1 mice, and that hyperinsulinemia is associated with adipogenic transition of hepatocytes. Among the adipocyte-associated genes in this program is PKM2, an anabolic enzyme implicated in tumorigenesis and the Warburg Effect. Viewed as a whole, our study implicates the existence of somatic parent-specific loci that may serve as useful biomarkers for metabolic risk profiling, and identifies new potential targets to improve insulin sensitivity and prevent NAFLD-associated HCC.

References

1.   James WP: WHO recognition of the global obesity epidemic, International journal of obesity (2005) 2008, 32 Suppl 7:S120-126

2.   Pender JR, Pories WJ: Epidemiology of obesity in the United States, Gastroenterology clinics of North America 2005, 34:1-7

3.   Hirsch HA, Iliopoulos D, Joshi A, Zhang Y, Jaeger SA, Bulyk M, Tsichlis PN, Shirley Liu X, Struhl K: A transcriptional signature and common gene networks link cancer with lipid metabolism and diverse human diseases, Cancer cell 2010, 17:348-361

4.   Ertle J, Dechene A, Sowa JP, Penndorf V, Herzer K, Kaiser G, Schlaak JF, Gerken G, Syn WK, Canbay A: Nonalcoholic fatty liver disease progresses to HCC in the absence of apparent cirrhosis, International journal of cancer 2010,

5.   El-Serag HB: Epidemiology of hepatocellular carcinoma in USA, Hepatol Res 2007, 37 Suppl 2:S88-94

6.   Williams CD, Stengel J, Asike MI, Torres DM, Shaw J, Contreras M, Landt CL, Harrison SA: Prevalence of nonalcoholic fatty liver disease and nonalcoholic steatohepatitis among a largely middle-aged population utilizing ultrasound and liver biopsy: a prospective study, Gastroenterology 2011, 140:124-131

7.   Christofk HR, Vander Heiden MG, Harris MH, Ramanathan A, Gerszten RE, Wei R, Fleming MD, Schreiber SL, Cantley LC: The M2 splice isoform of pyruvate kinase is important for cancer metabolism and tumour growth, Nature 2008, 452:230-233

8.   Fox JG, Dewhirst FE, Tully JG, Paster BJ, Yan L, Taylor NS, Collins MJ, Jr., Gorelick PL, Ward JM: Helicobacter hepaticus sp. nov., a microaerophilic bacterium isolated from livers and intestinal mucosal scrapings from mice, J Clin Microbiol 1994, 32:1238-1245.

9.   Rogers AB, Houghton J: Helicobacter-based mouse models of digestive system carcinogenesis, Methods in molecular biology (Clifton, NJ 2009, 511:267-295

10.   Stern SE, Williams K, Ferrannini E, DeFronzo RA, Bogardus C, Stern MP: Identification of individuals with insulin resistance using routine clinical measurements, Diabetes 2005, 54:333-339

11.   Rogers AB, Cormier KS, Fox JG: Thiol-reactive compounds prevent nonspecific antibody binding in immunohistochemistry, Lab Invest 2006, 86:526-533

12.   Boutin SR, Rogers AB, Shen Z, Fry RC, Love JA, Nambiar PR, Suerbaum S, Fox JG: Hepatic temporal gene expression profiling in Helicobacter hepaticus-infected A/JCr mice, Toxicologic pathology 2004, 32:678-693

13.   Rogers AB, Theve EJ, Feng Y, Fry RC, Taghizadeh K, Clapp KM, Boussahmain C, Cormier KS, Fox JG: Hepatocellular carcinoma associated with liver-gender disruption in male mice, Cancer research 2007, 67:11536-11546

14.   Amador-Noguez D, Yagi K, Venable S, Darlington G: Gene expression profile of long-lived Ames dwarf mice and Little mice, Aging Cell 2004, 3:423-441

15.   Kremer M, Perry AW, Milton RJ, Rippe RA, Wheeler MD, Hines IN: Pivotal role of Smad3 in a mouse model of T cell-mediated hepatitis, Hepatology (Baltimore, Md 2008, 47:113-126

16.   Lemke LB, Rogers AB, Nambiar PR, Fox JG: Obesity and non-insulin-dependent diabetes mellitus in Swiss-Webster mice associated with late-onset hepatocellular carcinoma, The Journal of endocrinology 2008, 199:21-32

17.   Bao B, Wang Z, Li Y, Kong D, Ali S, Banerjee S, Ahmad A, Sarkar FH: The complexities of obesity and diabetes with the development and progression of pancreatic cancer, Biochim Biophys Acta 2011, 1815:135-146

18.   Giouleme O, Diamantidis MD, Katsaros MG: Is diabetes a causal agent for colorectal cancer? Pathophysiological and molecular mechanisms, World journal of gastroenterology : WJG 2011, 17:444-448

19.   Rogers AB, Fox JG: Inflammation and Cancer. I. Rodent models of infectious gastrointestinal and liver cancer, American journal of physiology 2004, 286:G361-366

20.   Curley JP, Mashoodh R: Parent-of-origin and trans-generational germline influences on behavioral development: the interacting roles of mothers, fathers, and grandparents, Developmental psychobiology 2010, 52:312-330

21.   Singer JB, Hill AE, Burrage LC, Olszens KR, Song J, Justice M, O'Brien WE, Conti DV, Witte JS, Lander ES, Nadeau JH: Genetic dissection of complex traits with chromosome substitution strains of mice, Science (New York, NY 2004, 304:445-448

22.   Radonjic M, de Haan JR, van Erk MJ, van Dijk KW, van den Berg SA, de Groot PJ, Muller M, van Ommen B: Genome-wide mRNA expression analysis of hepatic adaptation to high-fat diets reveals switch from an inflammatory to steatotic transcriptional program, PloS one 2009, 4:e6646

23.   Goncalves LA, Vigario AM, Penha-Goncalves C: Improved isolation of murine hepatocytes for in vitro malaria liver stage studies, Malar J 2007, 6:169

24.   Das K, Das K, Mukherjee PS, Ghosh A, Ghosh S, Mridha AR, Dhibar T, Bhattacharya B, Bhattacharya D, Manna B, Dhali GK, Santra A, Chowdhury A: Nonobese population in a developing country has a high prevalence of nonalcoholic fatty liver and significant liver disease, Hepatology (Baltimore, Md 51:1593-1602

25.   Regimbeau JM, Colombat M, Mognol P, Durand F, Abdalla E, Degott C, Degos F, Farges O, Belghiti J: Obesity and diabetes as a risk factor for hepatocellular carcinoma, Liver Transpl 2004, 10:S69-73

26.   Donadon V, Balbi M, Ghersetti M, Grazioli S, Perciaccante A, Della Valentina G, Gardenal R, Dal Mas M, Casarin P, Zanette G, Miranda C: Antidiabetic therapy and increased risk of hepatocellular carcinoma in chronic liver disease, World journal of gastroenterology : WJG 2009, 15:2506-2511

27.   Chen TM, Lin CC, Huang PT, Wen CF: Metformin associated with lower mortality in diabetic patients with early stage hepatocellular carcinoma after radiofrequency ablation, Journal of gastroenterology and hepatology 2011, 26:858-865

28.   Kawaguchi T, Taniguchi E, Morita Y, Shirachi M, Tateishi I, Nagata E, Sata M: Association of exogenous insulin or sulphonylurea treatment with an increased incidence of hepatoma in patients with hepatitis C virus infection, Liver international : official journal of the International Association for the Study of the Liver 2010, 30:479-486

29.   Leiter EH: Selecting the "right" mouse model for metabolic syndrome and type 2 diabetes research, Methods in molecular biology (Clifton, NJ 2009, 560:1-17

30.   Leiter EH, Reifsnyder PC, Zhang W, Pan HJ, Xiao Q, Mistry J: Differential endocrine responses to rosiglitazone therapy in new mouse models of type 2 diabetes, Endocrinology 2006, 147:919-926

31.   Buchner DA, Burrage LC, Hill AE, Yazbek SN, O'Brien WE, Croniger CM, Nadeau JH: Resistance to diet-induced obesity in mice with a single substituted chromosome, Physiological genomics 2008, 35:116-122

32.   Millward CA, Burrage LC, Shao H, Sinasac DS, Kawasoe JH, Hill-Baskin AE, Ernest SR, Gornicka A, Hsieh CW, Pisano S, Nadeau JH, Croniger CM: Genetic factors for resistance to diet-induced obesity and associated metabolic traits on mouse chromosome 17, Mamm Genome 2009, 20:71-82

33.   Kong A, Steinthorsdottir V, Masson G, Thorleifsson G, Sulem P, Besenbacher S, Jonasdottir A, Sigurdsson A, Kristinsson KT, Jonasdottir A, Frigge ML, Gylfason A, Olason PI, Gudjonsson SA, Sverrisson S, Stacey SN, Sigurgeirsson B, Benediktsdottir KR, Sigurdsson H, Jonsson T, Benediktsson R, Olafsson JH, Johannsson OT, Hreidarsson AB, Sigurdsson G, Ferguson-Smith AC, Gudbjartsson DF, Thorsteinsdottir U, Stefansson K: Parental origin of sequence variants associated with complex diseases, Nature 2009, 462:868-874

34.   Sell H, Eckardt K, Taube A, Tews D, Gurgui M, Van Echten-Deckert G, Eckel J: Skeletal muscle insulin resistance induced by adipocyte-conditioned medium: underlying mechanisms and reversibility, Am J Physiol Endocrinol Metab 2008, 294:E1070-1077

35.   Yamada K, Noguchi T: Nutrient and hormonal regulation of pyruvate kinase gene expression, The Biochemical journal 1999, 337 (Pt 1):1-11

36.   Eckert DT, Zhang P, Collier JJ, O'Doherty RM, Scott DK: Detailed molecular analysis of the induction of the L-PK gene by glucose, Biochemical and biophysical research communications 2008, 372:131-136

37.   Tee LB, Kirilak Y, Huang WH, Smith PG, Morgan RH, Yeoh GC: Dual phenotypic expression of hepatocytes and bile ductular markers in developing and preneoplastic rat liver, Carcinogenesis 1996, 17:251-259

38.   Vander Heiden MG, Locasale JW, Swanson KD, Sharfi H, Heffron GJ, Amador-Noguez D, Christofk HR, Wagner G, Rabinowitz JD, Asara JM, Cantley LC: Evidence for an alternative glycolytic pathway in rapidly proliferating cells, Science (New York, NY 2010 , 329:1492-1499

39.   Asai Y, Yamada K, Watanabe T, Keng VW, Noguchi T: Insulin stimulates expression of the pyruvate kinase M gene in 3T3-L1 adipocytes, Bioscience, biotechnology, and biochemistry 2003, 67:1272-1277

40.   Li Y, Chang Y, Zhang L, Feng Q, Liu Z, Zhang Y, Zuo J, Meng Y, Fang F: High glucose upregulates pantothenate kinase 4 (PanK4) and thus affects M2-type pyruvate kinase (Pkm2), Molecular and cellular biochemistry 2005, 277:117-125

41.   Traxinger RR, Marshall S: Insulin regulation of pyruvate kinase activity in isolated adipocytes. Crucial role of glucose and the hexosamine biosynthesis pathway in the expression of insulin action, The Journal of biological chemistry 1992, 267:9718-9723

42.   Vander Heiden MG, Christofk HR, Schuman E, Subtelny AO, Sharfi H, Harlow EE, Xian J, Cantley LC: Identification of small molecule inhibitors of pyruvate kinase M2, Biochemical pharmacology 2010, 79:1118-1124

Table 1. Primer sequences for qRT-PCR.

Gene	Forward (5'-to-3')	Reverse (5'-to-3')	Region
Mitochondrial			
Cox1	TGGAGGCTTTGGAAACTGACTTG	GAGAAGGAGAAATGATGGTGGTAGG	325-436
Cytb	GGTGCCACAGTTATTACAAACCTCC	AGCGAAGAATCGGGTCAAGG	524-640
Nd1	CTTGTTCCCAGAGGTTCAAATCC	GGTTGTAAAATGCCGTATGGACC	67-243
Rnr2	CAAGAACCCCGCCTGTTTACC	GTTGGACCCTCGTTTAGCCG	926-1078
Imprinted			
Ctcf	TTTGTCACGCTCGGTTTACCC	TGCTGCTTTCGCAAGTGGAC	1500-1647
Dio3	CAACAGTGAAGGCGAGGAGATG	TGGGCTTGCTTGAAGAAATCC	260-391
Grb10	GGTTTTTCTCCGTTGTGACTCG	TTGGCTTCTTTGTTGTGGCG	231-378
H19	TGTGATGGAGAGGACAGAAGGG	CAGAGAGCAGCAGAGAAGTGTTAGC	972-1096
Igf2	TCGTGTTACCACCCAAAGACCC	GATGGAACTGTCCCTGCTCAAG	1701-1842
Igf2as	ATGAAGGGAAGGCTGGCTTG	CTGGTTTACAGGTCTGGTTTGAGC	571-699
Rtl1	AGCGACAGTTCAAACCAGTCAAG	CTCGTCATCTCCCAGGTCAGTATC	1042-1188
Sgce	GCAGTCAAGAAATGGAGCCTGTG	GCCACGAACTACTTCCTGATAGGTG	765-895
X-linked			
Arhgap6	TCCACTTTGACTACGAGGTCCCAC	AGGAACTGACGATGCTTGCG	594-722
Atp11c	TTGATGGACCTGTAGAAGGAGCC	CCCAAAAATGTGAACCCAAACC	1589-1691
Bgn	CGGATGATTGAGAATGGGAGCC	CCTTGGTGATGTTGTTGGAGTGC	941-1088
Bhlhb9	AAAGGGAAAGGTAAGGCAGGC	TCCTATGGTTGAAATCTGAGGTGC	266-413
Cd99l2	GGTCCCAAAAAGCCAAGTGC	GGTCATCGTTGCTGCCATAACC	313-442
Efnb1	AAGTGGCTTGTGGCTATGGTCG	GCTTGTCTCCAATCTTCGGGTAG	788-935
EG245643	TCTCTGCTTGGTTGAACGCAC	ATGCCCGAAGAATCAGTCAGG	1153-1293
Flna	TTCTCTGTCTGGTATGTCCCTGAAG	TCACTTTGCTGGCATCACCC	1122-1251
Gpc4	TCCTCCTCCTCCTTCACTACCAAC	ACCTTTAGGGGACAGAATGAGACC	315-442
Gyk	CCAAGAGAAGGATGGGTAGAACAAG	GCTGACACCAATGGCTTTGATG	458-589
Ikbkg	GCTGGTGGAGAAGAAGGAGTATTTG	TGGAGCAGGGAGTAAAGGAGGC	957-1110
Msn	GCGGTCCTGTTGGCTTCTTATG	CCTTGTTGAGTTTGTGCTGCTCC	551-683
Pdzd11	CCTATGAAAACCCTCCAGCGTG	AAATCCCAACTGAGCACCAGG	156-286
Praf2	AGAGCATCGGTCTAAAGCGGAC	AAAGGGTTGGTCTTGGGTATGG	475-613
Prdx4	CCTCTTCTTTCTGACCTGAACCATC	AACCAAACGCAGTGTCTCGTCCAC	622-795
Satl1	ACCTGCTGAGCCTGAAGATTGC	TGTCCCCAAAACCATCCCTG	1743-1867
Serpina7	TGTCTTGGTATTTGGGCTTCAGG	GAGTGGCATTTTGTTGGGGC	24-124
Slc25a5	GCCTGACTTCCTATCCTTTTGACAC	AAGCCTTGCTCCCTTCATCG	754-888
Stard8	TTGTTAGGTCTTGTCCCCAGCC	CACCCTTTTCTTTCCTCCTCAGAG	570-714
Sytl4	TCGGCGACTGAAGAATGAGC	CACACAAGTGCTGCTTTTGGG	293-428
Tceal8	GCAAAAGTCTTGTGACGAGAACG	ATGGCTCCCTTCAGTTTCCTCC	174-321
Tmsb4x	TGGCGAATCGTAATGAGGCG	TGATGTGAAAGGGGCAGCAC	351-500
Ubl4	TTCAGTGTAGCAGATGCCAGCAGG	CCCTTTTTCCATAGCCTCAGTCAC	383-526
Uty	AGATAGCCTCTGCCGCTTTCTC	GCCGCCATTTTCTTTTCCTC	251-351
Wdr40b	CCTTCAGCAACAAAAACCAGGAG	TTCTCACGGCAATAGGGCAG	1153-1273
Xlr3a	GGCTTTCTTTGACATTCTGCTCTG	CATCTTTCTTACTCGGGAGGTTTG	1074-1207
Xlr3b	ATCTTCTCCTGTCTTCCTCCTGTTC	AAAGCCTGCCATCTCTACCTGAG	843-976
Y-linked			
Uty	AGATAGCCTCTGCCGCTTTCTC	GCCGCCATTTTCTTTTCCTC	251-351
Other			
Acot10	AAATCACAGAAAGTCCTACCACCG	TCAAAGTCCTCAAGAATCCTGCC	311-456
Des	AACATCTCTGAGGCTGAAGAATGG	TCAATCTCGCAGGTGTAGGACTGG	933-1078
Egr1	TAATAGCAGCAGCAGCACCAGC	CAGAGCGATGTCAGAAAAGGACTC	562-703
Hnf3b	CACTGGGGACAAGGGAAATGAG	TTAGGGACACAGACAGGTGAGACTG	1624-1737
Hnf4a	TTCTGCGAACTCCTTCTGGATG	CGAGGGACGATGTAGTCATTGC	839-975
Hspb1	ACAGTGAAGACCAAGGAAGGCG	ACCTGGAGGGAGCGTGTATTTC	337-450
Ifng	AGCAAGGCGAAAAAGGATGC	AATCTCTTCCCCACCCCGAATCAG	453-625
Il1b	GTGAAATGCCACCTTTTGACAGTG	TGTTGATGTGCTGCTGCGAG	94-240
Il6	TGGAGCCCACCAAGAACGATAG	CACCAGCATCAGTCCCAAGAAG	109-208
Saa1	TTTGTTCACGAGGCTTTCCAAG	CCTTTGAGCAGCATCATAGTTCCC	103-228
Tnfa	GCAGGTTCTGTCCCTTTCACTCAC	TTCTGGAAGCCCCCCATCTTTTGG	95-233

Table 2. Top 10 up- and downregulated liver genes in AB6F1 versus B6AF1 males at 9 months as determined by microarray (mean signal density shown at right).

Symbol	Gene	Fold	AB6F1	B6AF1
Upregulated in AB6F1 males				
Sult2a2	sulfotransferase family 2A, dehydroepiandrosterone (DHEA)-preferring, member 2	239.98	10823	45
Kcnt2	Potassium channel, subfamily T, member 2	35.57	2367	67
Sult3a1	sulfotransferase family 3A, member 1	21.61	769	36
Cyp2b13	cytochrome P450, family 2, subfamily b, polypeptide 13	14.74	9501	645
Cfd	complement factor D (adipsin)	11.76	3807	324
Lcn2	lipocalin 2	11.68	3823	327
Thbs1	thrombospondin 1	8.51	403	47
Ly6d	lymphocyte antigen 6 complex, locus D	8.24	610	74
Saa2	serum amyloid A 2	8.18	4562	558
Orm2	orosomucoid 2	8.02	7225	901
Downregulated in AB6F1 males				
Slco1a1	solute carrier organic anion transporter family, member 1a1	-95.73	59	5682
Hsd3b5	hydroxy-delta-5-steroid dehydrogenase, 3 beta- and steroid delta-isomerase 5	-62.08	37	2272
Atp10a	ATPase, class V, type 10A	-14.30	4	55
Usp3	ubiquitin specific peptidase 3	-9.53	10	98
Clec2h	C-type lectin domain family 2, member h	-7.85	50	389
Serpine2	serine (or cysteine) peptidase inhibitor, clade E, member 2	-7.57	121	915
Evi5	Ecotropic viral integration site 5	-7.28	10	74
Susd4	sushi domain containing 4	-6.05	166	1003
Elovl3	elongation of very long chain fatty acids (FEN1/Elo2, SUR4/Elo3, yeast)-like 3	-5.58	2752	15358
Satl1	spermidine/spermine N1-acetyl transferase-like 1	-5.18	11	59

Table 3. Comparison of BW (g ± standard error of mean) and serum insulin (ng/dL) in A/J, B6.AX, B6.AY, B6AF1 and AB6F1 female (F) and male (M) mice on LF versus HF diet.

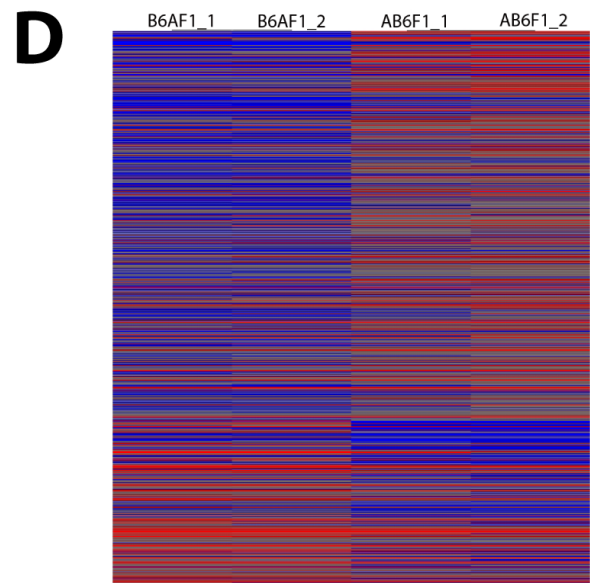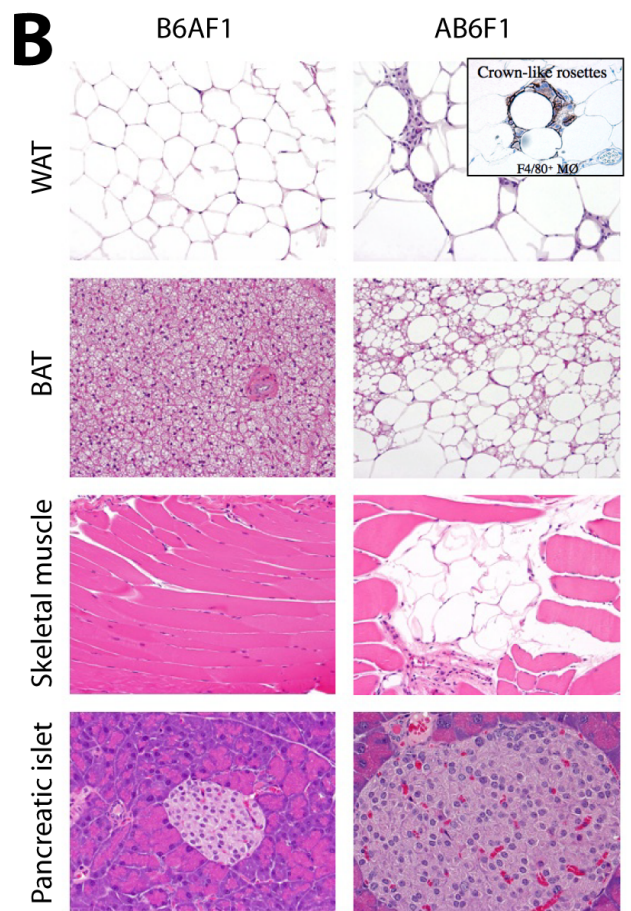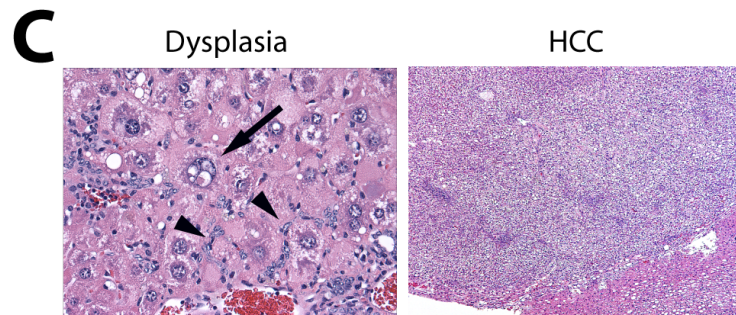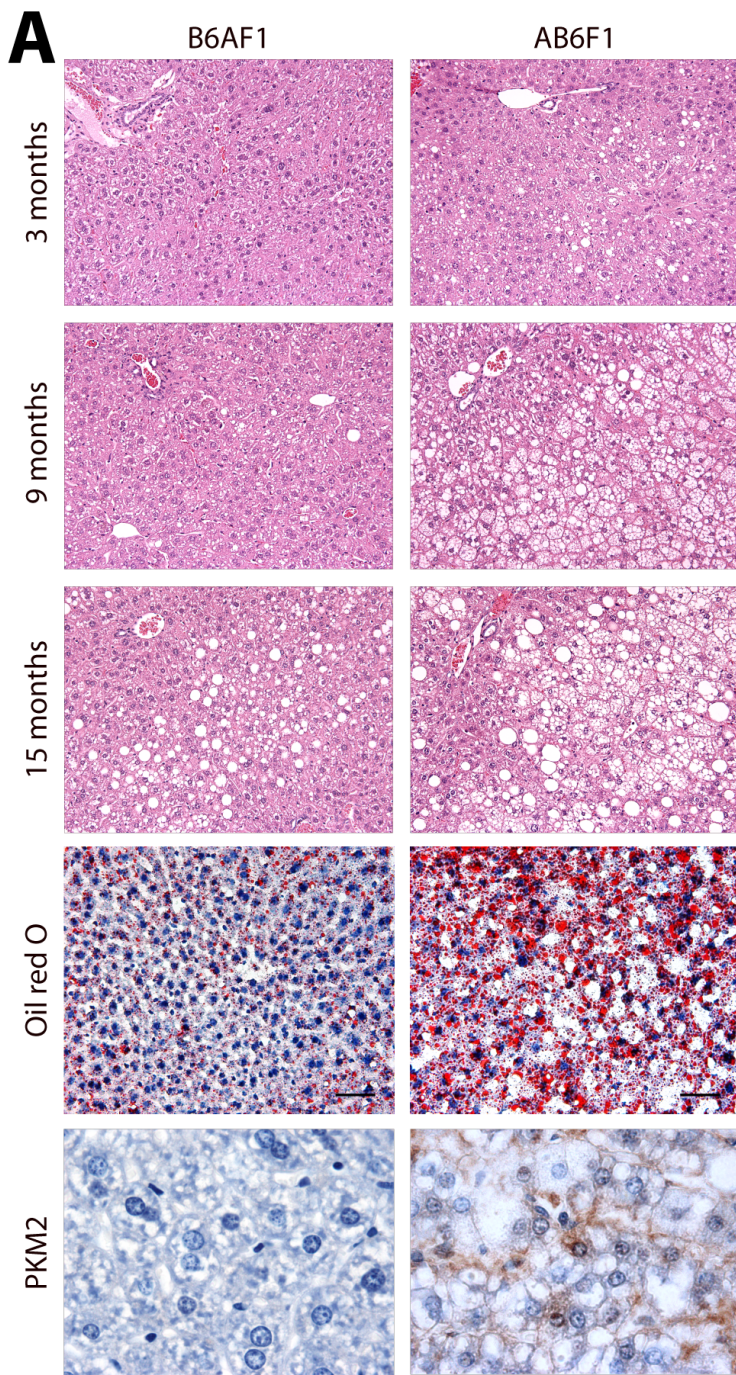|	A/J	B6.AX	B6.AY	B6AF1	AB6F1
F BW LF diet	23.0 ± 0.5	21.2 ± 0.7	21.0 ± 0.5	25.8 ± 1.2	26.9 ± 0.7
F BW HF diet	31.7 ± 1.4	30.0 ± 1.5	30.8 ± 2.3	39.0 ± 1.4	40.4 ± 3.3
F BW % incr.	38%	42%	47%	51%	51%
M BW LF diet	29.6 ± 0.7	26.7 ± 1.2	31.0 ± 0.8	34.6 ± 0.9	34.4 ± 1.2
M BW HF diet	37.4 ± 2.3	45.2 ± 1.1	46.9 ± 1.0	44.8 ± 0.9	46.8 ± 1.0
M BW % incr.	26%	69%	51%	29%	36%
F insulin LF diet	1.2 ± 0.3	1.2 ± 0.1	1.2 ± 0.1	1.2 ± 0.1	1.6 ± 0.4
F insulin HF diet	1.9 ± 0.7	2.4 ± 0.3	1.9 ± 0.3	3.7 ± 0.6	5.8 ± 1.1
F insulin % incr.	58%	200%	58%	308%	363%
M insulin LF diet	2.4 ± 0.3	1.6 ± 0.2	2.3 ± 0.2	4.0 ± 0.9	4.1 ± 0.8
M insulin HF diet	4.7 ± 0.3	9.6 ± 2.1	11.2 ± 2.2	6.8 ± 1.0	16.8 ± 1.3
M insulin % incr.	196%	600%	487%	170%	410%

Figure Legends

Figure 1. Clinical metabolic parameters in AB6F1 versus B6AF1 male mice. AB6F1 males developed early and progressive insulin resistance and hepatic steatosis (fatty liver). Although AB6F1 males also had moderately increased body mass compared with B6AF1 mice, neither morbid obesity nor hyperglycemia (not shown) were components of the phenotype. *$P < 0.05$ compared with age-matched B6AF1 mice.

Figure 2. Histopathologic and genomic comparison of AB6F1 versus B6AF1 males. (A) AB6F1 males exhibited more severe fatty liver lesions than B6AF1 males at all time points; lipid-filled vacuoles were verified by Oil Red O staining of frozen sections; immunohistochemical demonstration of PKM2 in AB6F1 neoplastic hepatocytes but not B6AF1 normal tissue. (B) AB6F1 liver demonstrating focus of cellular alteration and dysplasia characterized by marked pleomorphism, intranuclear pseudoinclusions (arrow), and oval cell hyperplasia (arrowheads; left); HCC arising on a background of metabolic hepatopathy (right). (C) Survey of non-hepatic insulin resistance-associated histologic lesions in AB6F1 males including WAT degeneration with MØ proliferation forming F4/80[+] crown-like rosettes, metaplasia of thoracic BAT to a WAT phenotype, focal skeletal muscle degeneration with fatty replacement, and pancreatic hyperplasia with occasional megaislets. (D) Microarray heat map demonstrating hierarchal clustering of AB6F1 versus B6AF1 males. (E) Histologic comparison of macrovesicular steatosis with WAT (top), and microvesicular steatosis with BAT (bottom), consistent with transcriptional alterations characteristic of adipogenic transition. Magnifications: (A) 100X except bottom row 400X; (B) 400X (left), 40X (right); (C) 200X; (E) 400X.
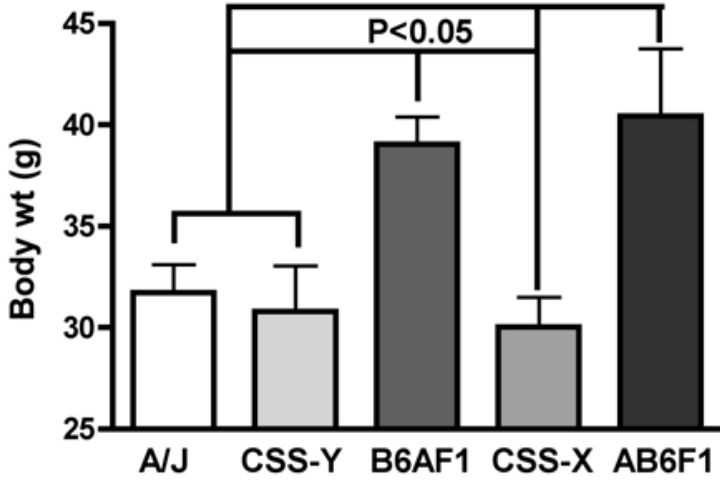
Figure 3. Serum insulin and body weight comparison between A/J, B6.AX, B6.AY, B6AF1 and AB6F1 mice on HF diet. Note dissociation between BW and serum insulin levels in F1 mice compared with other groups.

Figure 4. Primary hepatocyte isolation and culture. **(A)** Flow cytometry demonstrating <2% white blood cell (WBC) contamination of enriched hepatocyte population; ~25% of hepatocytes labeled with anti-CD95/Fas antibody. (B) MTT assay demonstrating strong trend (P=0.07) for increased viability of insulin-supplemented cells versus dexamethasone-alone after 4 days of culture. Photomicrographs demonstrate organization of hepatocytes into crude canaliculi, with increased clear (lipid) cytoplasmic vacuoles in insulin-supplemented cells; magnification 1000X. (C) qRT-PCR of insulin-supplemented primary hepatocytes (dark gray columns), especially on day 4 of culture, demonstrating increased expression of adipocyte-associated genes including vimentin, collagen 3α-1, fatty acid translocase (CD36), and pyruvate kinase M2 compared with non-supplemented cells (light gray columns); these genes also were upregulated in AB6F1 versus B6AF1 male mice at 15 months of age (black columns).
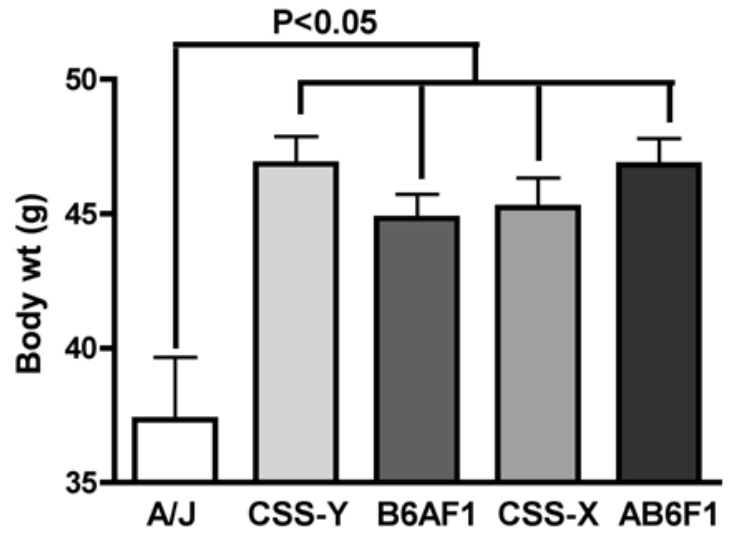
A

B6AF1 | AB6F1

3 months

9 months
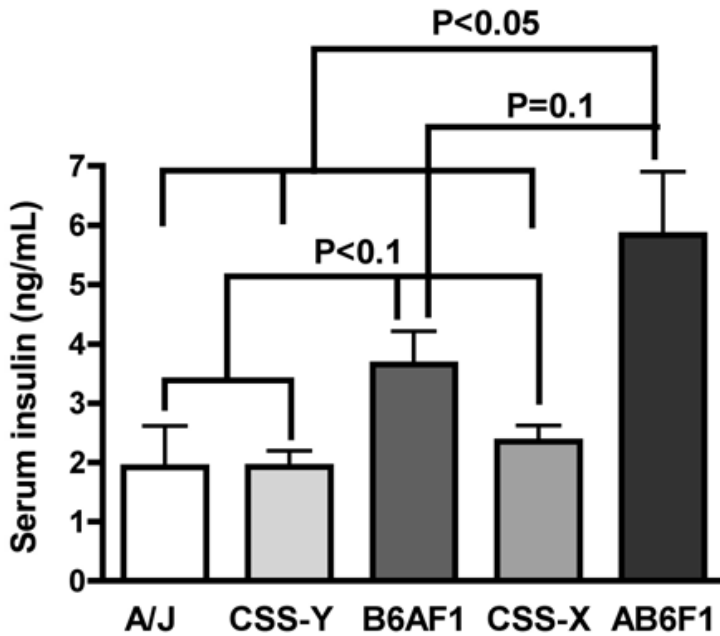
15 months

Oil red O

PKM2

B

B6AF1 | AB6F1

WAT

Crown-like rosettes
F4/80+ MØ

BAT

Skeletal muscle

Pancreatic islet

C

Dysplasia | HCC

D

B6AF1_1 B6AF1_2 AB6F1_1 AB6F1_2

E

Macrovesicular | WAT

Microvesicular | BAT

Female BW, high-fat diet

Body wt (g) — A/J, CSS-Y, B6AF1, CSS-X, AB6F1. P<0.05

Male BW, high-fat diet

Body wt (g) — A/J, CSS-Y, B6AF1, CSS-X, AB6F1. P<0.05

Female insulin, high-fat diet

Serum insulin (ng/mL) — A/J, CSS-Y, B6AF1, CSS-X, AB6F1. P<0.05, P=0.1, P<0.1

Male insulin, high-fat diet

Serum insulin (ng/mL) — A/J, CSS-Y, B6AF1, CSS-X, AB6F1. P<0.05